  Bull. Chem. Soc. Jpn., 55, 363—368 (1982)

Conformational Analysis of Intramolecular Excimer Formation in Dinaphthylalkanes

Shinzaburo Ito,* Masahide Yamamoto, and Yasunori Nishijima
Department of Polymer Chemistry, Kyoto University, Sakyo-ku, Kyoto 606
(Received March 23, 1981)

Intramolecular excimer formation processes were explained by the conformational energy calculated by an empirical method. Observed rate constants of excimer formation processes are closely correlated to the fraction of *tg* conformation. This indicates that intramolecular excimers are mainly formed by the internal rotation, *trans*→*gauche*, with reference to the naphthalene unit. The fraction of the *tg* conformation, which is an adjacent conformation to the excimer conformation on the conformational energy map, serves as an effective concentration of the intramolecular reaction. The small formation rate for *rac*-2,4-di(2-naphthyl)pentane is due to the unfavorable rotational mode ($g^+ \rightleftarrows g^-$) required to take the excimer conformation.

Since intramolecular excimers have been observed in various vinyl aromatic polymers and their dimer model compounds, it has become clear that the efficiency of excimer formation is greatly governed by the micro structures of molecules. Hirayama,[1] Longworth,[2] Chandross,[3] and Klöpffer[4] studied configurational requirements for the intramolecular excimer formation, and showed that the molecular structure in which two aromatic groups are separated with three carbon atoms of the methylene chain is the most favorable configuration for the intramolecular excimer formation. Their results show that the parallel sandwich arrangement of the aromatic groups is attainable with a propane chain, and that in the other type of compounds with shorter or longer chains than the propane chain, *e.g.*, ethane, butane, and pentane, two aromatic groups cannot approach each other owing to the conformational instability. This selectivity for the excimer formation in diarylalkanes is generally accepted as the $n=3$ rule.

Since we know that the intramolecular excimers are formed by the conformational relaxation after excitation of chromophores, the formation processes should be interpreted by the equilibrium conformations of the molecules and their internal rotation processes. For example, different efficiencies of the excimer formation even for the compounds holding $n=3$ rule, were reported by Hirayama,[1] and similar results were recently obtained by other workers.[5-7] These results suggest that there are some conformational factors controlling the intramolecular excimer formation besides the $n=3$ rule. But, in order to discuss the process of the intramolecular excimer formation in greater detail, quantitative data for the rate constant of the formation process are required.

In the preceding paper,[8] we reported a large difference in the efficiency of the excimer formation for the compounds satisfying the $n=3$ rule: 1,3-di(2-naphthyl)propane (1,3-DNPr), 1,3-di(2-naphthyl)butane (1,3-DNBu), *meso*-2,4-di(2-naphthyl)pentane (2,4-DNPe (*meso*)), and *rac*-2,4-di(2-naphthyl)pentane (2,4-DNPe (*rac*)). It was also shown by time-resolving measurements that the excimer formation rate constants change markedly with the molecular structures of the samples. We have tried to elucidate the internal rotation processes which lead to the intramolecular excimer formation.

In this paper, conformational energies of the four compounds mentioned above were calculated as functions of rotations about their C–C bonds, using an empirical treatment for the repulsive energies between nonbonded atoms and intrinsic torsional energies. The pathway of the internal rotation from the most stable conformation to the excimer conformation is discussed on the basis of the conformational energies. The observed rates of excimer formation are quantitatively well explained by these conformational analyses.

Procedures of the Calculation

The conformational energies of dinaphthylalkanes were calculated by using the conventional empirical method described in the preceding paper.[9] Potential energies due to the van der Waals interaction between nonbonded atoms and due to the intrinsic torsional potential energies associated with the rotation about the bonds are considered. For calculation of the van der Waals interaction, a potential function of Lennard-Jones type is used. The potential function is truncated by considering the molecule-solvent interaction according to Flory *et al.*[10,12] The total potential energy due to the van der Waals interaction is calculated as the sum over all pairs of nonbonded atoms. The intrinsic torsional potential energy for the skeletal alkane chain, $E(\phi)$, is calculated for the rotational angle ϕ, which is regarded as having a three fold periodicity:

$$E(\phi) = (E_0/2)\ (1-\cos 3\phi),$$

where E_0 is the torsional barrier energy, and is taken to be 12 kJ/mol.[11] The torsional energy for the rotation of naphthalene units, θ_i, is neglected, since the potential barrier is too low. The total potential energy is given by the sum of the potential energies due to the van der Waals interaction and the intrinsic torsional potentials.

The structural parameters used in this calculation are shown in Fig. 1. We must consider four independent angles to generate a given conformation of the dimers: two rotational angles, ϕ_1 and ϕ_2, for the chain skeleton and two rotational angles, θ_1 and θ_2, for the naphthyl groups, which are denoted as shown in Fig. 2. Angles are taken as 0 ° in the *trans* conformation. The naphthalene substituents are adopted as a reference conformation for the notation of *trans* and *gauche* conformations, in order to represent consistently the conformations of all

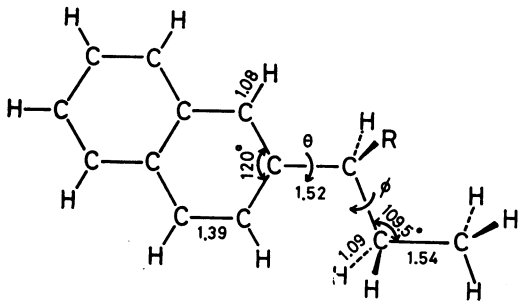

Fig. 1. Structural parameters of 1-(2-naphthyl)propane (R=H) and 2-(2-naphthyl)butane (R=CH_3).

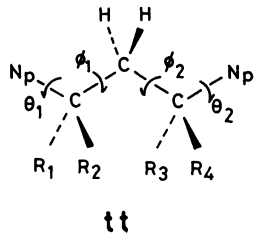

tt

Fig. 2. Dinaphthylalkanes in the *tt* conformation. 1,3-DNPr: (R_1=H, R_2=H, R_3=H, R_4=H), 1,3-DNBu: (R_1=H, R_2=H, R_3=CH_3, R_4=H), 2,4-DNPe(*meso*): (R_1=CH_3, R_2=H, R_3=CH_3, R_4=H), 2,4-DNPe(*rac*): (R_1=H, R_2=CH_3, R_3=CH_3, R_4=H). N_P=2-naphthyl.

compounds used in this study. For example, the *tt* conformation of 2,4-DNPe(*meso*), which is situated at (ϕ_1, ϕ_2)=(0°, 0°), represents the conformation in which two naphthalene units are extended at the ends of trimethylene chain as shown in Fig. 2, but this does not mean the planar zigzag conformation of the five skeletal carbon atoms.

Conformation maps should be drawn as a function of four angles: θ_1, ϕ_1, ϕ_2, and θ_2. But, in order to make the survey easier for the energy maps, they are drawn as a function of skeletal bond rotations ϕ_1 and ϕ_2. The other rotational angles, θ_1 and θ_2, are fixed on the angles to give a minimum energy at the most stable position of ϕ_1 and ϕ_2. For some specific region on the energy maps, the conformational energy is calculated as a function of all four angles, and the minimum energy was adopted. With the rotation of the skeletal angles, several stable conformations appear on the conformation maps. The fraction of i-th conformation f_i is calculated on the assumption that the distribution of conformations obeys the Boltzmann distribution including a weighting factor W_i,

$$f_i = \{W_i \exp(-E_i/RT)\}/\sum_i W_i \exp(-E_i/RT),$$

where E_i is the minimized potential energy for i-th conformation. The weighting factor is estimated by the 2-dimensional local energy maps for the rotation angles (θ_1, ϕ_1) and (θ_2, ϕ_2); here the values of one angle set are varied, holding the angles of the other set constant at the minimum position of the energy. In their local energy maps, the area surrounded by the contour which is 2.1 kJ/mol higher than the energy of each minimum is measured, and the weighting factor is calculated by $W_i=w_{1,i}\times w_{2,i}$, where $w_{1,i}$ and $w_{2,i}$ are proportional to calculated areas on the local energy maps for (θ_1, ϕ_1) and (θ_2, ϕ_2), respectively, corresponding to i-th conformation.

Conformational Energies

The calculation is carried out at first for 1-(2-naphthyl)propane (R=H in Fig. 1) and 2-(2-naphthyl)-butane (R=CH_3 in Fig. 1) which are the model compounds corresponding to the monomer units of dinaphthylalkanes. Conformational energy maps for these compounds are shown in Figs. 3 and 4, where

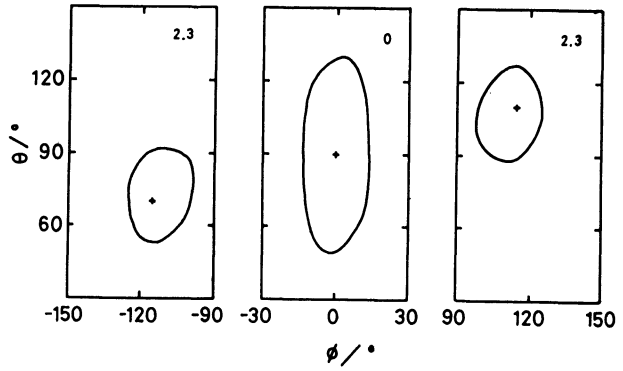

Fig. 3. Conformational energy maps of 1-(2-naphthyl)-propane. The energy minima are marked by+signs. The contour lines indicate the 2.1 kJ/mol higher energies than each minimum. Numerals in the figures show the potential energy at the minimum position in the unit of kJ/mol.

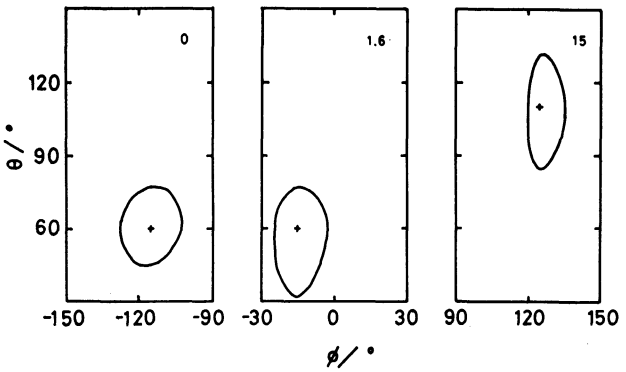

Fig. 4. Conformational energy maps of 2-(2-naphthyl)-butane.

the potential energies are calculated at intervals of 5° for each rotation angle. For 1-(2-naphthyl)propane, the potential minima are situated at (θ, ϕ)=(90°, 0°), (70°, −115°), and (110°, 115°). The potential minima for 2-(2-naphthyl)butane are found at (θ, ϕ)=(60°, −15°), (60°, −115°), and (110°, 125°). The stable conformations considerably deviate from the *trans* or *gauche* positions, owing to the repulsion between the methyl and naphthyl groups. The areas surrounded by the contour for each energy minimum differ significantly. The areas for the *trans* conformations are larger than that for *gauche* conformation; they are about 2.4 times or 1.2 times larger than the other potential

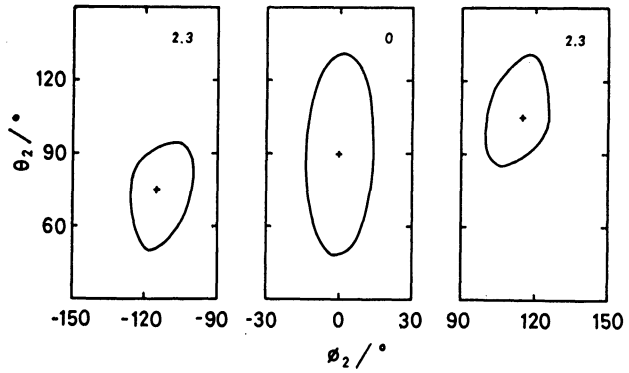

Fig. 5. Conformational energy maps of 1,3-DNPr as a function of θ_2 and ϕ_2, where θ_1 and ϕ_1 are fixed at *trans* position ($\theta_1=90°$, $\phi_1=0°$). Notations of the contour lines and numerals are the same as Fig. 3.

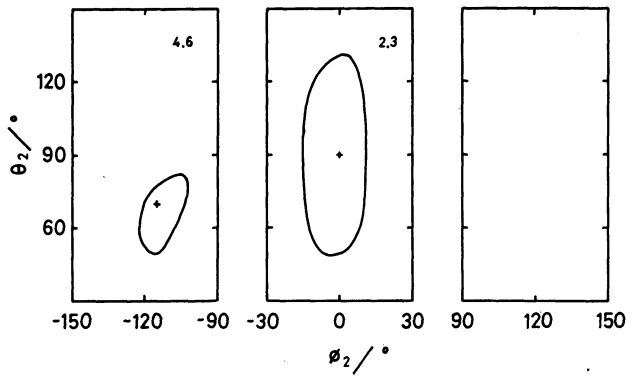

Fig. 6. Conformational energy maps of 1,3-DNPr as a function of θ_2 and ϕ_2, where θ_1 and ϕ_1 are fixed at *gauche* position ($\theta_1=70°$, $\phi_1=-115°$). Notations of the contour lines and numerals are the same as Fig. 3.

minima of 1-(2-naphthyl)propane or 2-(2-naphthyl)-butane, respectively. This must be reflected in the calculation of the fraction of each conformation. Next, the local energy maps as a function of θ_2 and ϕ_2 for the dimer compounds were calculated; in this calculations the angles θ_1 and ϕ_1 are held at the values obtained by the calculation for the monomeric model compounds. The local maps for 1,3-DNPr are shown in Figs. 5 and 6. The energy maps were calculated once more, by changing the rotational angle set to θ_1 and ϕ_1 and holding θ_2 and ϕ_2 to the minimum positions obtained on the previous maps. These procedures are repeated until the minimum position becomes consistent with that obtained on the previous map. For each stable conformation, the angles, minimized potential energy, weighting factor, and fraction of the conformation at 25 °C are listed in Tables 1, 2, and 3.

For 1,3-DNPr, the conformational energy map as a function of skeletal bond rotations, ϕ_1 and ϕ_2, is shown in Fig. 7, where the angles, θ_1 and θ_2 are fixed at $\theta_1=90°$ and $\theta_2=90°$. In this figure, a minimum position (*tt*) is marked by the symbol +, and the excimer conformations (g^+g^- and g^-g^+) are represented by the symbol ●. The most stable conformation is situated at *tt*, and is surrounded by four equivalent *tg* conformations. The potential energy of *tg* conformation is *ca.* 2.1 kJ/mol higher than that of *tt*. The minimized energy by the rotation of all angles at the important region of Fig. 7 is calculated. This result indicates that the barrier energies corresponding to the transitions of $tt \rightleftarrows tg$ and $tt \rightleftarrows g^+g^-$ ($tt \rightleftarrows g^-g^+$) are about 15 kJ/mol and 29 kJ/mol, respectively. These potential energies are caused mainly by the intrinsic torsional energies.

For 1,3-DNBu, the conformational energy map is shown in Fig. 8. The fixed angles θ_1 and θ_2 are chosen to be $\theta_1=90°$ and $\theta_2=120°$ for 1- and 3-naphthyl groups according to the result obtained from the local potential maps. The most stable conformation is found at tg^+, and metastable conformations appear at *tt*, g^-t, and g^+g^+. The barrier energy corresponding to the transition of $tt \rightleftarrows tg^+$ and $tt \rightleftarrows g^-g^+$ has the same values as that for 1,3-DNPr.

For 2,4-DNPe, conformational energy maps are shown

Table 1. Conformational energies and fractions of stable conformations in 1,3-DNPr

	θ_1/°	ϕ_1/°	ϕ_2/°	θ_2/°	W_t[a]	E_t / kJ mol^{-1}	f_t
tt	90	0	0	90	22	0	0.57
tg^+	90	0	115	105	10	2.3	0.10
tg^-	90	0	−115	75	10	2.3	0.10
g^+t	105	115	0	90	10	2.3	0.10
g^-t	75	−115	0	90	10	2.3	0.10
g^+g^+	110	115	115	110	1	4.6	0.01
g^-g^-	70	−115	−115	70	1	4.6	0.01

a) Weighting factors are given by the areas relative to the smallest one among the conformations.

Table 2. Conformational energies and fractions of stable conformations in 1,3-DNBu

	θ_1/°	ϕ_1/°	ϕ_2/°	θ_2/°	W_t[a]	E_t / kJ mol^{-1}	f_t
tt	90	0	15	120	5.0	1.3	0.35
tg^+	90	0	115	120	4.7	0	0.56
tg^-	90	5	−125	70	3.0	15	0.0
g^-t	70	−110	15	120	2.0	4.6	0.04
g^+g^+	110	115	115	120	1.0	2.1	0.05

a) Weighting factors are given by the areas relative to the smallest one among the conformations.

Table 3. Conformational energies and fractions of stable conformations in 2,4-DNPe

	θ_1/°	ϕ_1/°	ϕ_2/°	θ_2/°	W_t[a]	E_t / kJ mol^{-1}	f_t
meso							
tg^+	−120	−15	115	−120	4.4	0	0.49
g^-t	−120	−115	15	−120	4.4	0	0.49
g^-g^+	−120	−105	100	−120	1.0	4.6	0.02
racemo							
tt	−60	15	15	120	1.4	4.6	0.18
g^+g^+	−60	115	115	120	1.0	0	0.82

a) Weighting factors are given by the areas relative to the smallest one among the conformations.

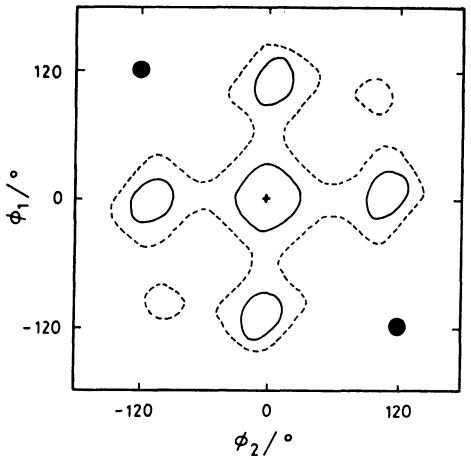

Fig. 7. Conformational energy map of 1,3-DNPr as a function of ϕ_1 and ϕ_2. The rotational angles of naphthalene units, θ_1 and θ_2 are fixed at $\theta_1=\theta_2=90°$. The most stable position and the excimer conformations are marked by the signs, + and ●, respectively. Solid lines indicate the 8.5 kJ/mol higher energy than the minimum. Broken lines show the 17 kJ/mol higher energy than the minimum.

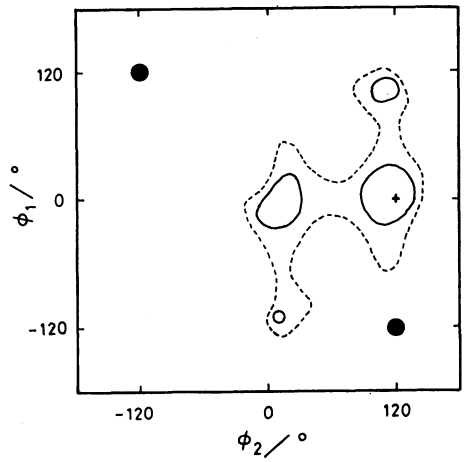

Fig. 8. Conformational energy map of 1,3-DNBu as a function of ϕ_1 and ϕ_2. The rotational angles of naphthalene units, θ_1 and θ_2 are fixed at $\theta_1=90°$, $\theta_2=120°$. Notations of the signs and lines are the same as Fig. 7.

in Fig. 9 for *meso* isomer and in Fig. 10 for *racemo* isomer. In these compounds, most of the conformations are unstable due to the steric hindrance of methyl substituents. Only two conformations are allowed: tg^+ and g^-t conformations for *meso* isomer, tt and g^+g^+ conformations for *racemo* isomer. In Fig. 9, a third potential minimum is observed besides the excimer conformation, g^-g^+, but its fraction is so small, as shown in Table 3, that it can be neglected.

Discussion

All rate constants in the photophysical kinetic scheme were reported in the previous paper. The observed excimer formation rate constant k_{21}, is shown again in Table 4. The values of k_{21} are much different for each

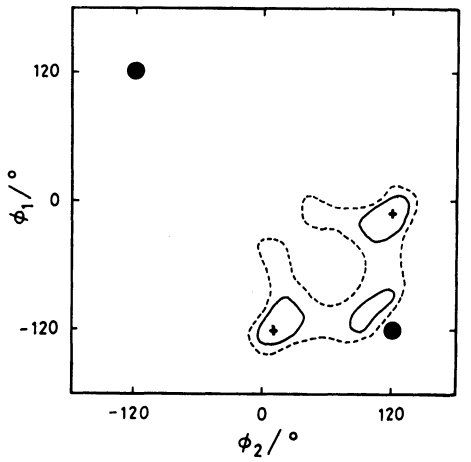

Fig. 9. Conformational energy map of 2,4-DNPe(*meso*). The rotational angles, θ_1 and θ_2 are fixed at $\theta_1=-120°$, $\theta_2=-120°$. Notations of the signs and lines are the same as Fig. 7.

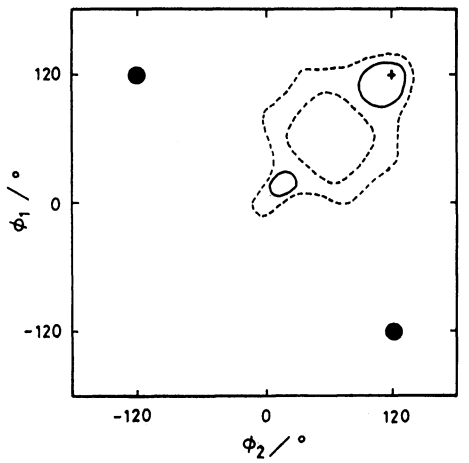

Fig. 10. Conformational energy map of 2,4-DNPe(*rac*). The rotational angles, θ_1 and θ_2 are fixed at $\theta_1=-60°$, $\theta_2=120°$. Notations of the signs and lines are the same as Fig. 7.

Table 4. Intramolecular excimer formation rate constants and their activation energies

	$k_{21}/10^7$ s^{-1}			
T/°C	1,3-DNPr	1,3-DNBu	2,4-DNPe	
			(*meso*)	(*rac*)
50	—	—	—	17
25	21	28	79	8.7
0	12	17	41	3.6
−2	4.8	7.0	17	—
−40	1.9	2.6	7.8	—
−60	0.7	1.0	3.3	—
E_a/kJ mol^{-1}	21	22	20	23

compound. In order to discuss the relationship between the excimer formation rate constants and the configuration of the compounds, it is necessary to follow the pathway of conformational changes on the potential

energy map for each compound.

In the ground state, the excimer conformation marked by ● is one of the unstable conformations, because of the steric hindrance of naphthalene units. However, in the excited state, this conformation is stabilized by the electronic interactions between two naphthalene units. The enthalpy change due to excimer formation is found to be *ca.* 19 kJ/mol for the intermolecular excimer formation in THF. This electronic interaction acts mainly in the parallel alignment of two naphthalene units.

The investigations on various dinaphthylalkanes have demonstrated the strict geometrical requirements for the attractive interaction in naphthalene chromophores.[3,13] The initial distribution of the molecular conformations at the instant of photo-excitation is the same as that in the ground state, and conformational relaxation to the excimer state occurs from the initial distribution. In the low temperature region, where the molecular motion is frozen, there is no indication of specific interaction between naphthalene chromophores. Hence, the relaxation processes will be discussed hereinafter on the assumption that there is no attractive interaction between two naphthalene units except in the excimer state.

For 1,3-DNPr, the conformational energy map shows that the *tt* position (0°, 0°) is the stable conformation where the naphthalene units are furthest apart from each other. Two excimer conformations, g^+g^- (g^-g^+), are equivalent in this compound. As for the pathway to the excimer conformations, the direct conformational changes from *tt* to g^+g^- (g^-g^+), are unfavorable, since such transitions require the co-operative motion of two rotational angles, ϕ_1 and ϕ_2; the calculated barrier energy is found to be 29 kJ/mol. This barrier comes from the intrinsic torsional potential. This value is higher than the activation energy observed for the excimer formation process: *ca.* 21 kJ/mol. Therefore, in order to reach the excimer conformations, it is necessary to pass through the *tg* conformations which are neighbors with both the stable *tt* and the excimer conformations. For the fraction of the *tg* conformation, a fairly large value is obtained: 0.4. The barrier energy for the conformational change from *tt* to *tg* is found to be 15 kJ/mol, and this value is sufficiently smaller than the observed activation energy of excimer formation. Hence, the appearance of *tg* conformations under the equilibrium, $tt \rightleftarrows tg$, contributes to the intramolecular excimer formation in 1,3-DNPr. The *tg* conformation can be considered as a precursory conformation of the intramolecular excimers.

For 1,3-DNBu, the energy map indicates that the most stable conformation is tg^+, which corresponds to the planar conformation of skeletal carbon atoms. The minimized energy for the *tt* conformation is 1.3 kJ/mol higher than that of lowest conformation *tg*, and the barrier energy for the transition from the *tt* conformation to the excimer state is the same as that of 1,3-DNPr: 29 kJ/mol. The fractions of the other conformations, except for tg^+ and *tt*, are negligibly small owing to the steric hindrance of the methyl substituent. In this compound, two excimer conformations, g^+g^- and g^-g^+ are not equivalent. The g^+g^- conformation which lies in the upper left-hand corner in Fig. 8, is unable to become an excimer site, since there is no available adjacent conformation to the excimer one. The intramolecular excimers in 1,3-DNBu, therefore, are formed at the g^-g^+ conformation. The sum of fractions for tg^+ and g^-t which are neighbors with the excimer site, is found to be 0.6. This predicts a larger excimer formation rate constant for 1,3-DNBu than that for 1,3-DNPr.

For 2,4-DNPe(*meso*), the calculation shows three potential minimum: tg^+ of lowest energy, its mirror image g^-t, and g^-g^+, which corresponds to the excimer conformation. Fractions of other conformations are rather small. The distribution is found predominantly in the tg^+ and g^-t forms, which are adjacent conformations to the excimer one, g^-g^+. There is a little fraction for the excimer conformation, g^-g^+ in the ground state. This rotational isomer was also found in the calculations of *meso*-2,4-diphenylpentane and its derivatives.[14,15] The fraction of this g^-g^+ conformation has been reported to be a few percent by NMR spectroscopy.[16] In this calculation, it was estimated to be 1—2% at 25 °C. If an appreciable fraction of 2,4-DNPe(*meso*) takes this conformation, a large component of excimer emission, rising immediately after the excitation pulse, should be observed in the time-resolving measurements. However, such a fast-rise component cannot be observed at all. Efficient intramolecular excimer formation is expected for 2,4-DNPe(*meso*), since a large portion of the molecules takes the adjacent conformations to the excimer state, g^-g^+. The other excimer conformation, g^+g^- can be neglected, because it has no available conformation for the excimer formation. Moreover, there is a steric hindrance between the two methyl substituents at this excimer state, g^+g^-.

The calculation for the three compounds: 1,3-DNPr, 1,3-DNBu, and 2,4-DNPe(*meso*), indicates that the intramolecular excimers are formed by the internal

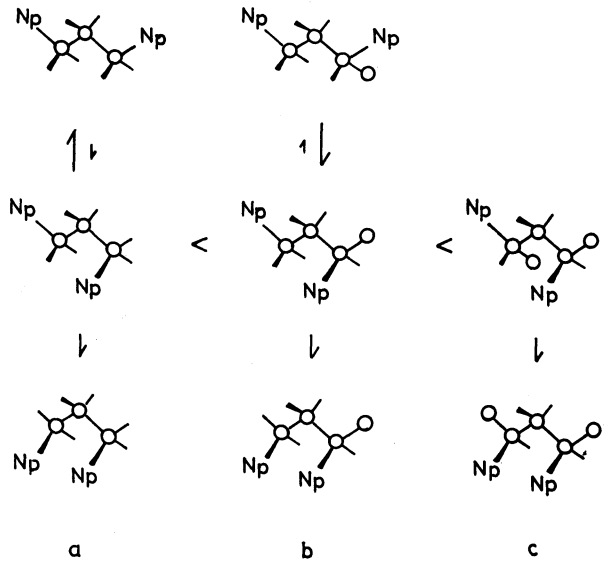

Fig. 11. Schematic illustration of excimer formation processes in dinaphthylalkanes. (a): 1,3-DNPr, (b) 1,3-DNBu, and (c) 2,4-DNPe(*meso*). N_P=2-naphthyl.

rotation, *trans→gauche* from the tg^+ or g^-t conformations, as shown in Fig. 11. Since the activation energies for the excimer formation processes are almost the same, the difference between the rate constants of the excimer formation is due to the frequency factors of their rate constants. These factors should be proportional to the fraction of the adjacent conformations, tg^+ and g^-t, if the intramolecular excimers are formed by the same rotational mode. Calculated fractions are 0.4 for 1,3-DNPr, 0.6 for 1,3-DNBu, and 0.98 for 2,4-DNPe(*meso*). These values are consistent with the results of excimer formation rate constants obtained experimentally: 2.1×10^8 s^{-1} for 1,3-DNPr, 2.8×10^8 s^{-1} for 1,3-DNBu, and 7.9×10^8 s^{-1} for 2,4-DNPe(*meso*). The somewhat larger value of 2,4-DNPe(*meso*) than that expected by the calculation may come from the existence of the metastable g^-g^+ conformation in the ground state, which slightly lowers the activation energy for the excimer formation process.

For 2,4-DNPe(*rac*), the situation is much different from that described above. Calculations reveal the lowest energy for the g^+g^+ form, which corresponds to the planar *trans* conformation of the skeletal five carbon atoms, and which is also a neighbor with the excimer conformation. However, the internal rotations, $g^+g^+\rightleftarrows g^+g^-$ ($g^+g^+\rightleftarrows g^-g^+$) are required for the excimer formation. This transition is a different type of rotation from that of the other three compounds. It is known that the barrier to the interconversion of *gauche* forms, $g^+\rightleftarrows g^-$ is higher than that between *t* and *g* forms; the barrier energy has been reported to be *ca.* 27 kJ/mol.[17] On the route to the excimer state, it is also possible to take the tg^+ (g^+t) conformations. But these conformations are unstable because of the steric hindrance, and the imposed energy is 13—17 kJ/mol.[16] Moreover, the *trans→gauche* transition to the excimer conformation ($tg^+\rightarrow g^-g^+$ or $g^+t\rightarrow g^+g^-$) becomes a $g^+\rightleftarrows g^-$ transition with reference to the methyl groups. Thus, for 2,4-DNPe(*rac*), the interconversion $g^+\rightleftarrows g^-$ is necessary in the case of either rotation in order to reach the excimer site. The small value of the formation rate constant (8.7×10^7 s^{-1}) and the somewhat higher activation energy (23 kJ/mol) obtained for this compound is not determined by the fraction of the adjacent conformation but by the different transition mode of the internal rotation.

Our calculation did not include the interaction energy in the electronically excited state. However, the rate of intramolecular excimer formation can be interpreted reasonably by this conformational analysis. The agreement between the observed rate constants and the results of calculations indicates that the formation of intramolecular excimers are determined by the internal rotation, *trans→gauche*, and that the fraction of the *tg* conformation, which is an adjacent conformation to the excimer one, serves as an effective concentration in the intramolecular reaction.

References

1) F. Hirayama, *J. Chem. Phys.*, **42**, 3163 (1965).
2) J. W. Longworth and F. A. Bovey, *Biopolymers*, **4**, 1115 (1966).
3) E. A. Chandross and C. J. Dempster, *J. Am. Chem. Soc.*, **92**, 3586 (1970).
4) W. Klöpffer, *Ber. Bunsenges. Phys. Chem.*, **74**, 693 (1970).
5) R. S. Davidson and T. D. Whelan, *J. Chem. Soc., Chem. Commun.*, **1977**, 361.
6) L. Bokobza, B. Jasse, and L. Monnerie, *Eur. Polym. J.*, **13**, 921 (1977).
7) M. Goldenberg, J. Emert, and H. Morawetz, *J. Am. Chem. Soc.*, **100**, 7171 (1978).
8) S. Ito, M. Yamamoto, and Y. Nishijima, *Bull. Chem. Soc. Jpn.*, **54**, 35 (1981).
9) T. Kanaya, Y. Hatano, M. Yamamoto, and Y. Nishijima, *Bull. Chem. Soc. Jpn.*, **52**, 2079 (1979).
10) D. A. Brant and P. J. Flory, *J. Am. Chem. Soc.*, **87**, 2791 (1965).
11) A. Abe, R. L. Jernigan, and P. J. Flory, *J. Am. Chem. Soc.*, **88**, 631 (1966).
12) D. Y. Yoon, P. R. Sundararajan, and P. J. Flory, *Macromolecules*, **8**, 776 (1975).
13) S. Ito, M. Yamamoto, and Y. Nishijima, *Rep. Prog. Polym. Phys. Jpn.*, **22**, 453 (1979).
14) S. Gorin and L. Monnerie, *J. Chim. Phys. Phys.-Chim. Biol.*, **67**, 869 (1970).
15) B. Froelich, B. Jasse, C. Noel, and L. Monnerie, *J. Chem. Soc., Faraday Trans. 2*, **74**, 445 (1978).
16) T. Moritani and Y. Fujiwara, *J. Chem. Phys.*, **59**, 1175 (1973).
17) J. E. Piercy and M. G. S. Rao, *J. Chem. Phys.*, **46**, 3951 (1967).